Available online at www.sciencedirect.com

SCIENCE DIRECT®

Remote Sensing of Environment 96 (2005) 399 – 408

Remote Sensing of Environment

www.elsevier.com/locate/rse

Retrieval of evapotranspiration over the Alpilles/ReSeDA experimental site using airborne POLDER sensor and a thermal camera

M. Gómez[a,1], A. Olioso[b,*], J. A. Sobrino[a,1], F. Jacob[c]

[a]Department of Thermodynamics, Faculty of Physics, University of Valencia, 50 Dr. Moliner, 46100 Burjassot, Spain
[b]INRA CSE, Domaine Saint-Paul, Site Agroparc, 84914, Avignon Cedex 9, France
[c]ESA PURPAN, 75 voie du TOEC, 31076 Toulouse Cedex 3, France

Received 8 October 2004; received in revised form 22 March 2005; accepted 25 March 2005

Abstract

Knowledge of land surface evapotranspiration is of prime interest for environmental applications, such as optimizing irrigation water use, especially in arid and semiarid rangelands where water shortage is a critical problem. Numerous methods aiming at estimating evapotranspiration have been proposed in the literature. In the current paper, we assess the potential of the evaporative fraction based on the S-SEBI (Simplified Surface Energy Balance Index) concept for estimating instantaneous evapotranspiration, and extend this potential to the retrieval of daily evapotranspiration (ET_d). To this end, a feasible and operational method is developed, which allows mapping instantaneous and daily evapotranspiration over the Alpilles ReSeDA (Remote Sensing Data Assimilation) experimental area. The method is implemented using data collected with two airborne sensors: PolDER (Polarization and Directionality of Earth Reflectance) and a Thermal camera. The validation over test sites shows that daily evapotranspiration can be obtained within an error of 1 mmd^{-1}. Finally a daily evapotranspiration image for the Alpilles ReSeDA experimental site is presented.

Keywords: Evapotranspiration; Latent heat flux; Net radiation flux; Soil heat flux; ReSeDA; S-SEBI

1. Introduction

Detailed knowledge of land surface fluxes, especially latent and sensible components, is of prime interest for environmental applications: monitoring land surface climate, evaluating parameterization schemes for weather and climatic models (Van der Hurk et al., 1997) and scheduling irrigation for optimizing agricultural practises (Bastiaanssen & Chandrapala, 2003; Bastiaanssen et al., 2000; Panda et al., 2003). Amongst these applications daily evapotranspiration is an important parameter for monitoring water requirements of crops and water consumption from field to regional scale (Bastiaanssen et al., 2000). Integrated evapotranspiration through the whole phenological cycle is also closely related to crop final productivity (Ines et al., 2002). For operational applications, water managers and irrigation engineers need accurate estimations of surface fluxes in a spatially distributed manner, and especially of evapotranspiration (ET). The main methods classically used to measure ET are available at the field scale (Bowen ratio, eddy correlation system, soil water balance), but do not allow estimating surface fluxes when dealing with large spatial scales. Nowadays, numerous countries use the recommended FAO 56 method (Allen et al., 1998), which consists of estimating crop evapotranspiration using a reference evapotranspiration and a crop coefficient. The reference evapotranspiration is retrieved using the Penman–Monteith method, and corresponds to a grazing land under optimum soil moisture conditions. Then, the surface

* Corresponding author. Tel.: +33 4 3272 24 06; fax: +33 4 3272 2362.
E-mail addresses: monica.gomez@uv.es (M. Gómez), olioso@avignon.inra.fr (A. Olioso), Sobrino@uv.es (J.A. Sobrino), frederic.jacob@esa-purpan.fr (F. Jacob).
[1] Fax: +34 96 3543115.

0034-4257/$ - see front matter © 2005 Elsevier Inc. All rights reserved.
doi:10.1016/j.rse.2005.03.006

canopy resistance is set to a constant value by considering grass as a single big leaf (Allen et al., 1998). Crop surface evapotranspiration under non-standard conditions is finally adjusted using both a water stress coefficient and a crop coefficient. However, surface resistance depends on the day, the weather conditions, especially available radiation and vapor pressure deficit (Ortega-Farias et al., 2004). The determination of crop coefficients is also debatable because it depends on several environmental factors.

Over the last years, the scientific community has been interested in estimating evapotranspiration by remote sensing, since it is the unique way to retrieve ET at several temporal and spatial scales. To this end, different methods have been developed to derive surface fluxes from remote sensing observations. It is always difficult to classify these methods, since their complexities depend on the balance between the used empirical and physical based modules (Courault et al., 2005). One type of methods is the residual of the energy budget which combines empirical relationships and physical modules, such as SEBAL (Surface Energy Balance Algorithm for Land, Bastiaanssen, 2000; Bastiaanssen et al., 1998a,b; Jacob et al., 2002c), S-SEBI (Simplified Surface Energy Balance Index, Roerink et al., 2000), SEBS (Surface Energy Balance System, Jia et al., 2003; Su, 2002), and TSEB (Two-Source Energy Balance, French et al., 2003; Kustas & Norman, 1999; Norman et al., 1995). Amongst these methods, we focused in this study on the S-SEBI model which is a simple way to derive evapotranspiration from evaporative fraction based on the contrast between dry and wet areas. The S-SEBI concept was previously applied to Landsat images for the estimation of instantaneous fluxes (Roerink et al., 2000). In the present paper, we assessed the S-SEBI concept to the retrieval of instantaneous evapotranspiration, and further extended it to the retrieval of daily evapotranspiration. This was performed over the Alpilles experimental area near Avignon (South-East of France) in the framework of the ReSeDA (Remote Sensing Data Assimilation) program (Baret et al, 2002). The ReSeDA database is characterized by high spatial resolution and multitemporal remote sensing data, with a better retrieval of models inputs through the use of multispectral and multidirectional remote sensing information.

The current paper is structured as following:

1. We present the modeling background of the study, by focusing on the evaporative fraction based on S-SEBI concept.
2. We briefly describe the experimental setup of the Alpilles ReSeDA program, by focusing on the remote sensing and field data to be used.
3. We present the method implementation over the ReSeDA database.
4. Finally, the validation results are presented, discussed and enhanced against a sensitivity analysis for the S-SEBI key points: the results are analyzed and discussed considering instantaneous latent heat flux at the data acquisition time, and especially evapotranspiration integrated over the diurnal cycle.

2. Model

2.1. Instantaneous evapotranspiration

The S-SEBI model is based on the energy balance equation and allows the estimation of the instantaneous latent heat flux $\mathrm{LET_i}$ ($\mathrm{Wm^{-2}}$) according to:

$$\mathrm{LET_i} = \Lambda_i(R_{ni} - G_i) \quad (1)$$

where Λ_i is the instantaneous evaporative fraction (adimentional), R_{ni} is the instantaneous net radiation flux ($\mathrm{Wm^{-2}}$) and G_i is the instantaneous soil heat flux ($\mathrm{Wm^{-2}}$). The instantaneous net radiation flux can be obtained according to Hurtado and Sobrino (2001):

$$R_{ni} = (1-\alpha)R_{c\lambda\downarrow} + \varepsilon R_{g\lambda\downarrow} - \varepsilon\sigma T_S^4 \quad (2)$$

where α is the albedo, $R_{c\lambda\downarrow}$ is the incoming shortwave radiation ($\mathrm{Wm^{-2}}$), $R_{g\lambda\downarrow}$ is the incoming longwave radiation ($\mathrm{Wm^{-2}}$), σ ($\mathrm{Wm^{-2}\,K^{-4}}$) is the Stefan Boltzman constant, ε is the surface emissivity, and T_S is the surface temperature (K). The soil heat flux (G_i) can be derived from both net radiation R_{ni} and LAI (Leaf Area Index) according to Choudhury et al. (1987):

$$G_i = 0.4R_{ni}\exp(-0.5\ \mathrm{LAI}). \quad (3)$$

The critical point for solving Eq. (1) is estimating Λ_i. Previous works in the literature focused on the retrieval of evaporative fraction from remote sensing (see the review by Bastiaanssen, 2000). In the current work we determine Λ_i according to:

$$\Lambda_i = \frac{T_H - T_s}{T_H - T_{LE}} \quad (4)$$

where T_S is the land surface temperature and T_H and T_{LE} are the temperatures corresponding to dry and wet conditions for a given albedo value (see Fig. 1). Roerink et al. (2000) noted that Eq. (4) is only applicable when:

- The atmospheric conditions are constant over the images.
- The study site includes simultaneously wet and dry areas, with large occurrences for both.

From Fig. 1 we observe the following trends:

1. An approximately constant surface temperature (T_S) for low albedo values, related to water saturated surfaces like open water and irrigated lands, where all available energy is used for evapotranspiration process.

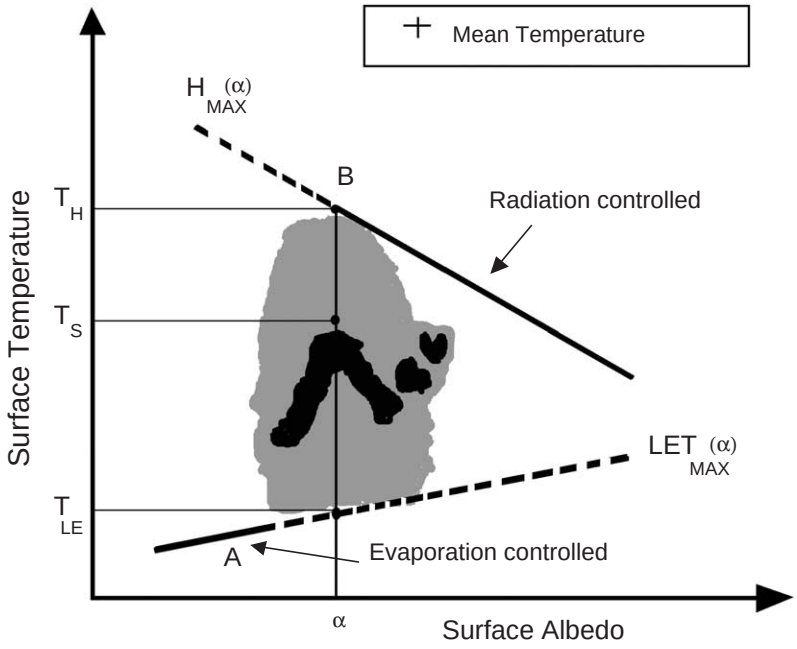

Fig. 1. Feature space plot of albedo and surface temperature for Alpilles (12-03-97) (adapted from Roerink et al., 2000), overlaid with the two albedo-to-temperature relationships for $LET_{max}(\alpha)$ ("wet surfaces") and $H_{max}(\alpha)$ ("dry surfaces") and the mean surface temperature per albedo unit.

2. An increase of T_S with albedo increase from A to B points. Indeed, less soil moisture availability yields an evapotranspiration decrease and therefore a surface temperature increase. Here surface is said to be "evaporation controlled".
3. Finally, surface temperature from B to largest albedo values. These results from soil moisture decrease such as no evaporation can occur: all available energy is used for surface heating. Thus an albedo increase yields a net radiation decrease and therefore less surface heating. Here, surface temperature is said to be "radiation controlled".

For a given albedo value, the variation of surface temperature between the wet and dry lines is mainly related to variations in land surface water availability. Thus, it is possible to define a wet temperature T_{LE} obtained when instantaneous sensible heat flux $H_i=0$ which induces $LET_{max\ i}(\alpha)=R_{ni}-G_i$; and a dry temperature T_H when $LET_i=0$ which induces $H_{max\ i}(\alpha)=R_{ni}-G_i$.

2.2. Daily evapotranspiration

One of the study objectives is to extend the S-SEBI concept to retrieval of daily evapotranspiration ET_d (in mmd^{-1}). For this, latent heat flux must be integrated over the whole day, and converted to ET_d by accounting for the latent heat of vaporization ($L=2.45$ MJ kg^{-1}). As LET_i is only derived once a day from remote sensing images, this integration will be done by assuming that the evaporative fraction at the daily scale is similar to that derived instantaneously from Eq. (4) at time of remote sensing data acquisition (Bastiaanssen, 2000). Thus writing Eq. (1) for daily and instantaneous values yields the following equation:

$$\frac{LET_d}{LET_i}=\frac{\Lambda_d}{\Lambda_i}\frac{(R_{nd}-G_d)}{(R_{ni}-G_i)}\approx\frac{(R_{nd}-G_d)}{(R_{ni}-G_i)}. \quad (5)$$

Then ET_d may be obtained as:

$$ET_d=LET_i\frac{R_{nd}}{L(R_{ni}-G_i)} \quad (6)$$

where R_{nd} (W m^{-2}) and R_{ni} are the daily and instantaneous net radiation flux respectively. The hypothesis of a daily ground heat flux close to zero was also done for deriving Eq. (6) (Seguin & Itier, 1983). The change from instantaneous to daily values for net radiation may be performed using the ratio between both values ($C_{di}=R_{nd}/R_{ni}$). In this way Eq. (6) can be rewritten as:

$$ET_d=\frac{\Lambda_d R_{nd}}{L}=\frac{\Lambda_i C_{di} R_{ni}}{L}. \quad (7)$$

According to Seguin and Itier (1983) $C_{di}=0.30\pm0.03$. However, Wassenaar et al. (2002) showed that this ratio depends on solar zenith angle and varies between 0.05 and 0.3 following a sinusoidal law from winter to summer (assuming R_{ni} was obtained at noon). It is then possible to derive different values of C_{di} along the year.

At this point, it should also be noted that it is not necessary to calculate the soil heat flux to estimate the daily evapotranspiration, although, it is required for estimating instantaneous latent heat flux.

3. Experimental data and application of the model

This section reports the data acquisition in the framework of the Alpilles/ReSeDA experiment. We considered airborne remote sensing data for the S-SEBI model implementation, and field data for the validation exercise. The Alpilles/ReSeDA experiment was the first part of the ReSeDA program, which aimed at improving the use of multi-temporal, multispectral and multidirectional remote sensing data for their assimilation into land surface process modes (Baret, 2000; Prévot et al., 1998). Besides, the simultaneous collection of remote sensing data at different spatial resolution allows addressing scaling issues (Olioso et al., 1998). This experiment took place from October, 1996 to November 1997, over a 5 by 5 km^2 Mediterranean agricultural region including 200 by 200 m^2 fields (see Fig. 2), with corn, alfalfa, wheat and sunflower as main crops.

3.1. Field data

A detailed description of the field experimental setup can be found in Olioso et al. (2002a). The Alpilles/ReSeDA experiment performed continuous monitoring over several agricultural fields of:

1. Surface radiative variables: emissivity, temperature and albedo,
2. Vegetation characteristics: height, biomass distribution and LAI,
3. Standard meteorological variables: wind speed, air humidity/temperature, atmospheric/solar incident radiations and rainfall,
4. Soil characteristics and water balance: temperature, moisture and water pressure profiles, hydrodynamic parameters, surface soil moisture, surface roughness and surface dry bulk density,
5. Surface energy balance components: net radiation, soil heat flux, sensible and latent heat flux.

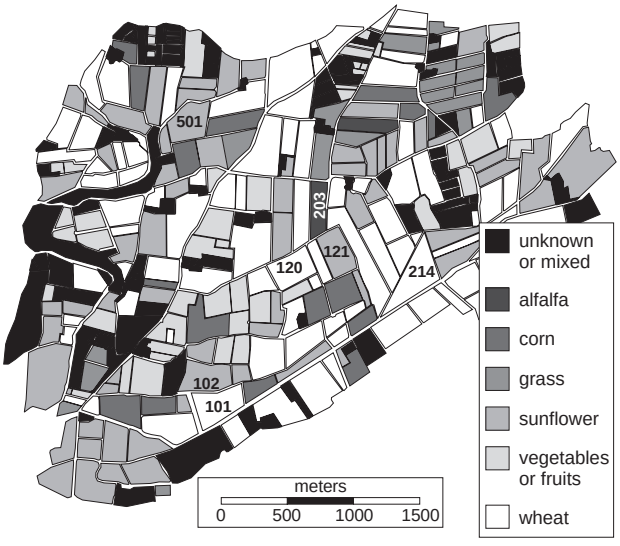

Fig. 2. Land use map of Alpilles experimental site in 1997. Different measurements were done on the numbered fields (101: wheat, 102: sunflower, 120: wheat, 121: sunflower, 203: alfalfa, 214: wheat and 501: sunflower).

Meteorological measurements were performed at the center of the experimental site over bare soil. Surface energy fluxes were measured as following:

- Shortwave incoming radiation was measured over the whole solar spectrum with Kipp and Zonen pyranometer. Longwave incoming radiation was measured over the thermal domain with an Eppley pyrgeometer. For both incoming radiation measurements, the error was around 5%.
- Net radiation measurements were performed using Rebs (Radiation and energy balance systems, Inc.) Q7 instruments and Crouzet-INRA devices set at 3 m height (over wheat and alfalfa fields) or 6 m height (over sunflower fields).
- Ground heat flux was measured using heat flow transducers Rebs HFT-1 and HFT 3.1, installed 5 cm deep. A correction was applied for accounting of heat storage between the sensor level and the soil surface from soil temperature and soil moisture measurements at 2.5 cm.
- Sensible and latent heat fluxes were computed from two measurement levels of air temperature and relative humidity, by using the Bowen ratio method (see Cellier & Olioso, 1993; Olioso et al., 2002a). Sensible heat flux was occasionally acquired using a 1D sonic anemometer Campbell CA27.

All these data were acquired with a 15 second time step and a 20-min period averaging.

3.2. Optical remote sensing data

The optical remote sensing data were acquired over the experimental site using both an airborne thermal infrared camera (INFRAMETRICS 760) and the airborne PolDER (Polarization and Directionality of Earth Reflectance) sensor over the Alpilles region (see Fig. 2) in the framework of the ReSeDA project (Jacob et al., 2002c). These data were collected around solar noon, during 19 days between March and October 1997, with a frequency about once to twice a month. The two sensors were set up on board a PIPER PA28 ARROW4 aircraft. Both instruments flew on clear sky days approximately at 3000 m altitude yielding 20 m of nadir spatial resolution. The standard image size is 250 lines × 250 samples covering a 5 by 5 km zone.

The airborne PolDER imaging radiometer collected Vis-NIR measurements over four bands centered at 443, 550, 670, 865 nm, each 40 nm wide. The zenith view angles ranged between 0° and 50°. The sensor calibration was performed by the Laboratoire d'Optique Atmosphérique (Lille, France) three times: before,

during and after the experiment. It accounted for ambient temperature, dark current, optic transmission, and the relative sensitivity of the CCD matrix detectors. The INFRAMETRICS 760 thermal video camera performed Thermal Infra Red (TIR) measurements over the [7.25–13.25] μm range, with view zenith angles ranging from 0° to 40° thanks to a wide-angle lens. The sensor was instrumentally characterized once after the experiment. This characterization accounted for the influence of the ambient temperature on the sensor radiometric sensitivity, and for both the directional sensitivity and the geometrical distortions induced by the use of a wide-angle lens.

4. Model implementation

This section reports the implementation of the S-SEBI model from the optical remote sensing data collected during the ReSeDA experiment. From these data, we computed surface variables to be next used as model inputs, in order to obtain model simulations.

4.1. Computing model inputs

Fig. 3 shows the flowchart of the methodology proposed to estimate the evapotranspiration in the Alpilles test site from the S-SEBI concept. According to this figure, it is necessary to make radiometric and geometric corrections for the computation of surface variables. The images were geometrically matched according to a Lambert II projection using data acquired by both global positioning system and gyroscopic central unit set up aboard the plane. The atmospheric corrections for PolDER imaging radiometer were performed using the SMAC algorithm along with climatological data and field measurements of atmospheric variables (see Leroy et al., 2000). The atmospheric corrections for INFRAMETRICS 760 were performed using the radiative transfer code MODTRAN 3.5 along with its climatological database and radio soundings launched from a meteorological station located at 30 km toward the west of the experimental site (Gu et al., 2000; Jacob et al., 2003). Once the correction has been carried out we can estimate the different input data which are necessary to estimate evapotranspiration according to S-SEBI concept.

PolDER images provided BRDF (Bidirectional Reflectance Distribution Function) angular samplings in the four considered channels. These angular samplings were next fitted by BRDF models such as Li-Ross or Walthall (Jacob et al., 2002a). From these fittings, images of hemispherical and nadir reflectances were computed. Hemispherical reflectance in all the channels were linearly combined to obtain albedo with an accuracy about 0.017 (Jacob et al., 2002b). Fitted hemispherical and nadir reflectances were also used for retrieving LAI maps using a neural network based procedure developed by Weiss et al. (2002). The accuracy of LAI retrievals was evaluated through a comparison against field measurements, which gave a RMSE (Root Mean Square Error) of 0.49. Emissivity images were derived from LAI images using the following relationship adapted from François et al. (1997):

$$\varepsilon = 1 - \exp(-1.325\mathrm{LAI})\left(1 - \varepsilon_g\right) - \alpha'(1 - \exp(-1.325\mathrm{LAI}))(1 - \varepsilon_v) \quad (8)$$

where ε_g is the soil emissivity, ε_v is the leaf emissivity, α' is the cavity effect coefficient, and LAI is the leaf area

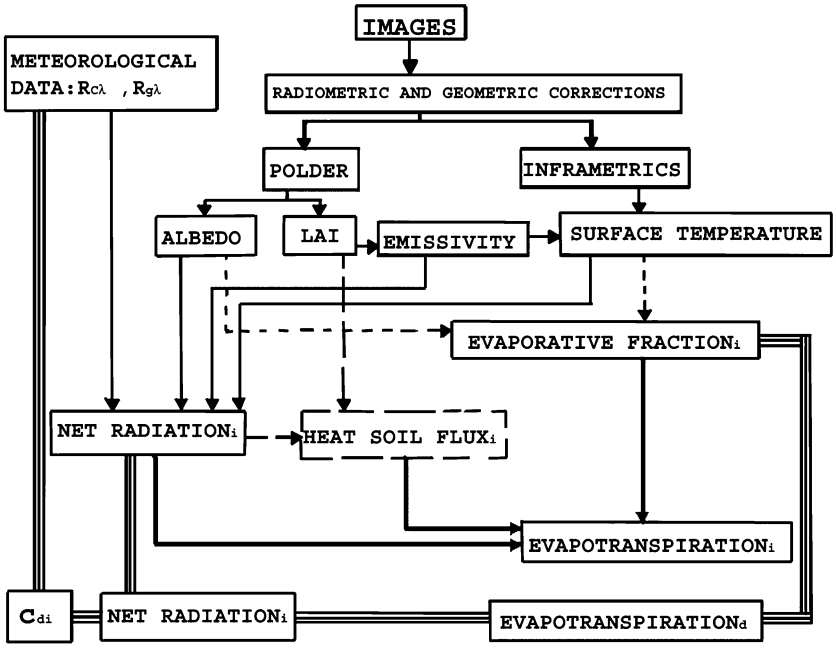

Fig. 3. Flowchart of the methodology proposed to estimate the instantaneous and daily evapotranspiration in the Alpiles test site.

Table 1
Equations of T_H and T_{LE} (K) for the different flights carried out over the Alpilles site

DOE	UTC (hh:mm:ss)	T_H (K)	T_{LE} (K)	C_{di}
437	12:07:47	−20 α+312	7.5 α+286	0.176
451	11:56:25	−30 α+318	7.5 α+285	0.205
466	10:40:13	−35 α+323	7.5 α+285	0.278
472	10:50:21	−50 α+330	5 α+281	0.209
474	11:20:12	−35 α+323	7.5 α+286	0.259
487	12:03:36	−42.5 α+333	7.5 α+289	0.263
488	13:28:39	−27.5 α+322	7.5 α+292	0.291
501	12:31:28	−30 α+326	5 α+293	0.265
508	10:31:46	−40 α+330	5 α+290	0.264
526	11:51:00	−37.5 α+336	7.5 α+296	0.293
529	11:20:30	−40 α+338	10 α+294	0.295
541	12:43:08	−40 α+330	5 α+291	0.255
555	11:49:12	−47.5 α+345	22.5 α+287	0.293
575	11:42:04	−65 α+360	7.5 α+294	0.289
576	12:49:57	−65 α+360	5 α+294	0.287
613	12:12:42	−57.5 α+355	7.5 α+295	0.255
627	11:20:39	−25 α+323	7.5 α+293	0.233

DOE is the number of days since 1996, January 1st and α represents the albedo. The table also includes the time and the C_{di} coefficients.

index. The basis for choosing the values for soil and leaf emissivities was the ground based measurements collected on the Alpilles test site (Coll et al., 2002). Due to the measurements made on ε_V and ε_g, this equation allowed estimating emissivity with a standard deviation around 0.01.

To derive surface radiometric temperature, it was necessary to convert surface brightness temperature by accounting for effects of both surface emissivity and atmospheric radiation in the INFRAMETRICS waveband. We used the procedure proposed by Olioso (1995), who expressed the surface temperature as a function of the brightness temperature, the emissivity and the atmospheric radiation. The error in the surface temperature determination using this procedure ranged between ±0.6 and 0.9 K, depending on T_s.

4.2. Obtaining instantaneous and daily evapotranspiration

According to Fig. 3 and assuming that albedo, emissivity and surface temperature are known, we can calculate the different fluxes that allow the estimation of the evapotranspiration. First, we calculate the instantaneous net radiation flux (R_{ni}) according to Eq. (2). To obtain the instantaneous soil heat flux we apply Eq. (3). Finally it is necessary to calculate the evaporative fraction (Λ_i) (see Fig. 1 and Eq. (4)). The equations $T_H = a_H\alpha + b_H$ and $T_{LE} = a_{LE}\ \alpha + b_{LE}$ obtained for each image are given in Table 1. At this stage, we are able to compute instantaneous evapotranspiration. Finally, daily values of evapotranspiration are obtained by applying Eq. (7) in which the C_{di} coefficient is computed at the image acquisition time (see Table 1).

5. Results

5.1. Daily evapotranspiration map

Once the S-SEBI method was implemented over the Alpilles/ReSeDA database, it was possible to generate maps of instantaneous and daily evapotranspiration over the experimental area. Fig. 4 displays the daily evapotranspiration map on March, 12th, 1997. The larger values (2–3 mmd^{-1}) are obtained for wheat (central part of the image) and on evergreen forest (lower part of the image), intermediate (1–2 mmd^{-1}) for wheat, alfalfa and grass fields and the lowest for sunflower, corn and spring wheat. These results are in agreement with the knowledge we have on phenological stages for the various crops in the area. Thus, at the image time, the most developed crops were wheat, grass and alfalfa, while spring wheat was just sown and sunflower and corn were not yet sown. The obtained values were also close to field measurements. Assessing the proposed methodology was performed through a validation against field measurements for R_{ni} Eq. (2), G_i Eq. (3), LET_i Eq. (1) and ET_d Eq. (7). Validation scatter plots are displayed in Figs. 5, 6, 7 and 8. The corresponding RMSE values are 40 Wm^{-2} (7%), 48 Wm^{-2} (40%), 90 Wm^{-2} (26%) and 1 mmd^{-1} for R_{ni}, G_i, LET_i and ET_d, respectively. Figs. 5 and 6 also show that R_{ni} and G_i, were usually overestimated (BIAS=16 and 35 Wm^{-2}, respectively), while latent heat flux and ET_d, whereas more scattered,

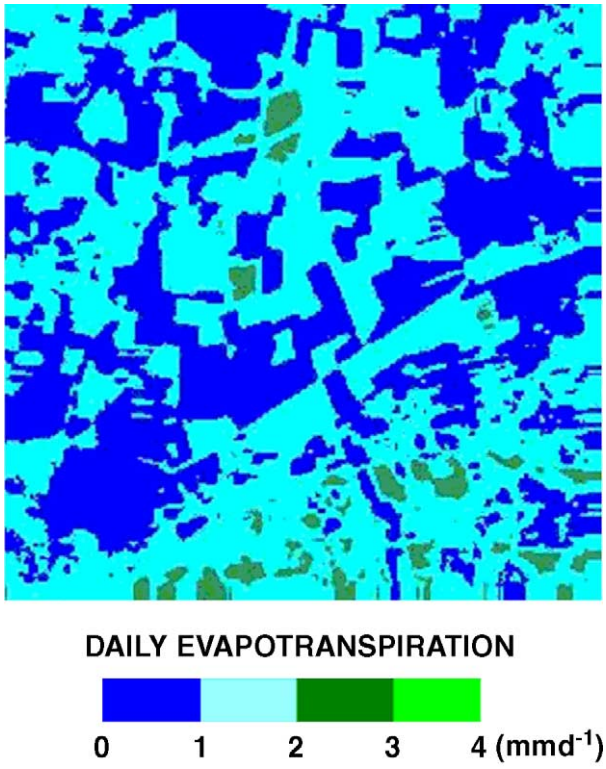

Fig. 4. Daily evapotranspiration map (mmd^{-1}) from Alpilles site (March, 12th at 12 hours GMT). The image covers a 5 by 5 km area.

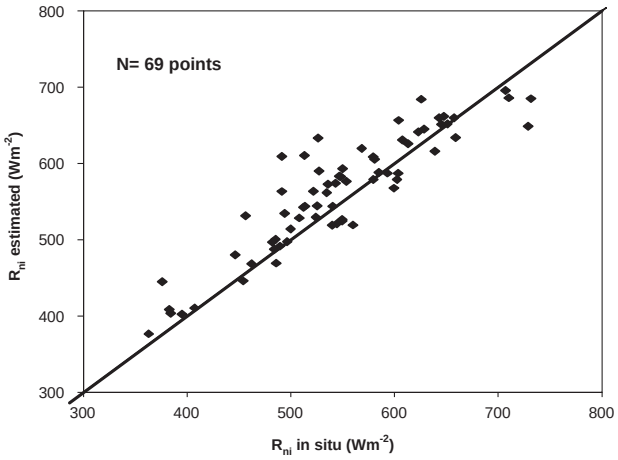

Fig. 5. Comparison, against field measurements, of S-SEBI net radiation products (N indicates the number of field measurements carried out in the instrumented fields). The graph includes the 1:1 line.

were rather unbiased (BIAS = 2 Wm^{-2} and 0.2 mmd^{-1}, respectively).

5.2. Sensitivity analysis

A sensitivity analysis was performed in order to assess the effect of errors in deriving S-SEBI inputs on evapotranspiration calculations. To estimate the error in daily evapotranspiration it is necessary to obtain the errors in R_{ni} and in the evaporative fraction. The error in C_{di}, around 0.02, was not considered because it is negligible in comparison with the other errors. The error in R_{ni} is 7% approximately; this error was obtained by applying the error theory to Eq. (2) in which we considered, from the validation exercises over the whole Alpilles experimental site, the following RMSE for the parameters included in Eq. (2): 0.017 for albedo, 0.9 K for T_S, 0.01 for ε and 5% for $R_{c\lambda\downarrow}$ and $R_{g\lambda\downarrow}$.

The estimation of Λ_i error is the critical point of the sensitivity analysis. This is due to the fact that T_H and T_{LE} should be obtained from a graphical procedure which may generate significant errors. To evaluate these errors, we plot

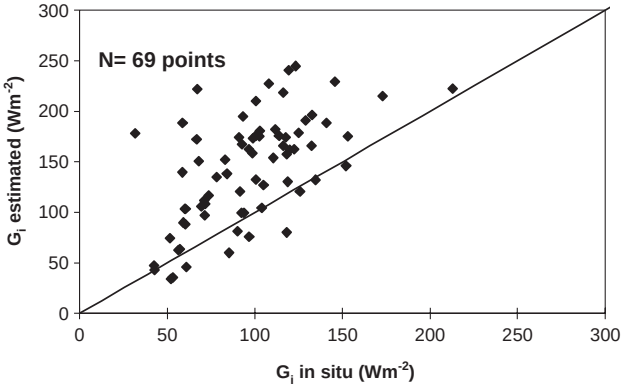

Fig. 6. Similar to Fig. 4, for the instantaneous soil heat flux.

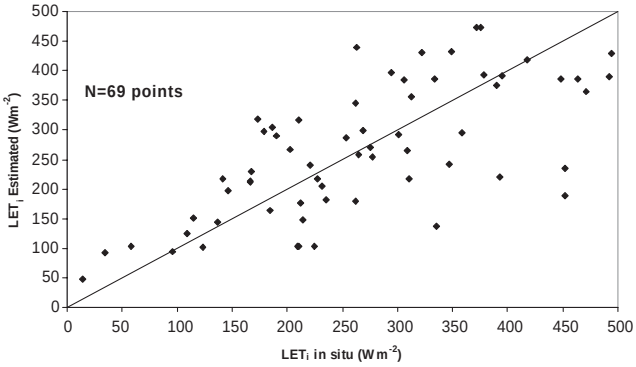

Fig. 7. Similar to Fig. 5, for the instantaneous latent heat flux.

in Fig. 9 T_S versus albedo for the whole Alpilles areas on the 12th of March 1997 at 12h GMT (Day Of Experiment, DOE, 437 in the Alpilles notation which considers the number of days since the 1996 January 1st). From the figure it is clearly shown that in an ideal situation in which T_H and T_{LE} are obtained without error (this is represented by A in the figure) and in terms of the absolute value, the slope of the straight line that define T_H, whose value in the considered image is 7 K approximately, is lower than the slope of T_H (around 35 K). Besides, it should be noted that the graphical determination of T_{LE} is easier than that of T_H. This is due to the clear and compact distribution of the points for the lowest T_S values (287 K in the figure); while T_H determination is more critical due to the scarce points for the largest T_S values (308 K in the figure). In this context, a quantitative error estimation of Eq. (4) is not easy. In this paper, we have evaluated the error considering the more frequent situations that occur in the graphical determination of T_H and T_{LE}. These situations have been based in our practical experience. Thus, assuming a frequent situation, represented by B in Fig. 9 (remember that A represent the ideal situation), in which the slopes of T_H and T_{LE} can reach an error of 15% and 70%, respectively, the evaporative fraction is obtained with an error of 20% approximately. This implies an error of 1 mmd^{-1} in the daily evapotrans-

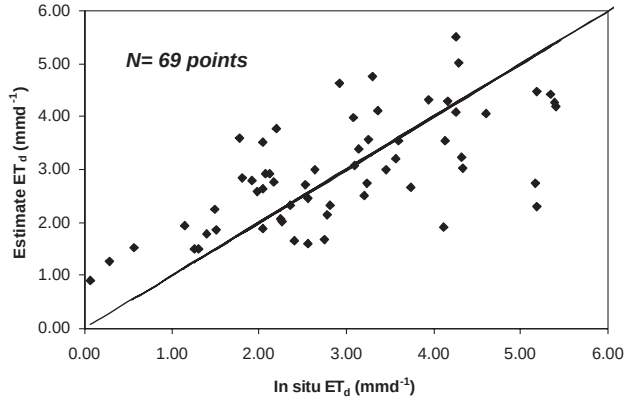

Fig. 8. Daily evapotranspiration estimated in function of measured values. The graph includes the 1:1 line.

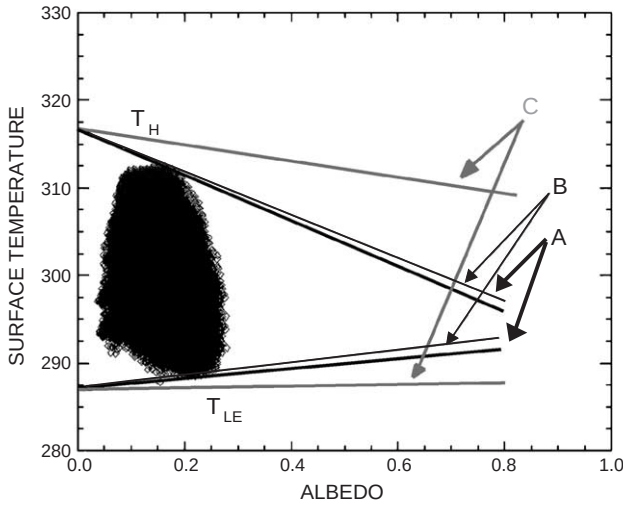

Fig. 9. Plot of surface temperature versus albedo for the 12 March at 12:00 GMT. The straight lines that represent T_H and T_{LE} are included in the figure. (A) represents a precise determination of these lines without error, while (B) was obtained considering an error of 15% and 70%, and (C) 60% and 70%, in the slopes of T_H and T_{LE}, respectively.

piration, error that is similar to the one obtained in Section 5.1 from the validation. Similarly for an extreme situation in which the T_H slope error is around 60% (represented by C in Fig. 9), the daily evapotranspiration is obtained with an error of 1.2 mmd^{-1}.

6. Discussion

The proposed methodology allows the determination of daily evapotranspiration with an error of 1 mmd^{-1}; however the principal disadvantage of the methodology is that the studied images must contain extreme surface values of temperature. On the other hand, errors in net radiation estimations may be related to the errors in albedo estimations. Thus, Fig. 1 in Jacob et al. (2002b), showed that some underestimation of albedo occurred which may result in net radiation slight overestimation we obtained in the present study. Errors in the estimation of ground heat flux (Fig. 6) may be (at least partly) related to the error in net radiation; it must be noticed that errors in R_{ni} and G_i cancelled each other in the calculations of instantaneous latent heat flux. The scattering obtained when comparing evapotranspiration estimations to measurements (see Fig. 8) may be mainly related to the scattering in $R_{ni}-G_i$ and to the determination of evaporative fraction. Actually, the sensitivity analysis demonstrated that errors in the determination of T_H and T_{LE} lines, and therefore in Λ_i, appeared having a major impact on the estimation of evapotranspiration. This is the most critical point in the proposed methodology. Other methods such as SEBAL were applied in the Alpilles test site (Jacob et al., 2002c). The results showed that the relative errors for the different fluxes (4.1% for net radiation flux, 47.8% for heat soil flux, and 33.1% for the latent heat flux) were not very different from those obtained in the present study with S-SEBI, even if SEBAL results were slightly better than S-SEBI in the current study. One of the main differences between S-SEBI and SEBAL relied on the used concept which is not considering H flux computation, aerodynamic and thermal roughness are not considered. From this comparison, it looks like using the simpler method as S-SEBI is not problematic in terms of evapotranspiration retrieval accuracy. On the other hand, computations from SEBAL or similar models are required when seeking the maps of sensible heat flux. Further, it is very important to note that determining roughness length is a difficult task, and that no classical remote sensing method has been proven to be accurate enough for retrieving well this variable. Olioso et al. (2002b) performed a sensitivity analysis of several sensible heat flux models applied to the same dataset, showing that in the context of the Alpilles experiment, the problem of estimating roughness was the most limiting factor for obtaining accurate results on sensible heat flux estimation.

7. Conclusions

In this paper we extend and evaluate the S-SEBI concept to map the daily evapotranspiration over the Alpilles experimental site in the framework of the ReSeDA program using two airborne sensors; the PolDER and a thermal camera. In comparison with the field data, the proposed methodology allows the estimation of R_{ni}, G_i, LET_i and ET_d with an error of 40 Wm^{-2}, 48 Wm^{-2}, 90 Wm^{-2} and 1 mmd^{-1}, respectively.

The principal disadvantage of the methodology is that the studied images must contain extreme values of surface temperature. However in the comparison with other methods such as SEBAL similar results have been obtained. This supposed a clear advantage, because S-SEBI is a simpler method that is not problematic in terms of evapotranspiration retrieval accuracy, while, computations from SEBAL or similar models need to determine roughness length which is a difficult task, and that no classical remote sensing method has been proven to be accurate enough for retrieving well this variable.

Acknowledgements

The Alpilles/ReSeDA project was funded by the EEC-DG XII (contract ENV4-CT96-0326-PL952071) and the French Programme National de Télédétection Spatiale and Programme National de Recherches en Hydrologie. We would also like to thank the European Union (EAGLE, Project SST3-CT-2003-502057), and the Ministerio de Ciencia y Tecnología (Project REN2001-3105/CLI) for the financial support.

References

Allen, R. G., Pereira, L. S., Raes, D., & Smith, M. (1998). Crop evapotranspiration: Guidelines for computing crop water requirements. *FAO irrigation and drainage paper*, *vol. 56.* Rome: FAO, 300pp.

Baret, F. (2000). ReSeDA, Assimilation of multisensor and multitemporal remote sensing data to monitor soil and vegetation functioning. *Final Report, EC Research Project, 2000*. (http://www.avignon.inra.fr/reseda/base/documents/reseda-report/00reseda-report.pdf)

Baret, F. (Ed.) (2002). Special issue: Multi-sensor and multi-temporal remote sensing observations to characterise canopy functioning. The ReSeDA project. *Agronomie*, *vol. 22 (6)*, 165 pp.

Bastiaanssen, W. G. M. (2000). SEBAL-based sensible and latent heat fluxes in the irrigated Gediz Basin, Turkey. *Journal of Hydrology*, *229*, 87–100.

Bastiaanssen, W. G. M., & Chandrapala, L. (2003). Water balance variability across Sri Lanka for assessing agricultural and environmental water use. *Agricultural and Water Management*, *58*, 171–192.

Bastiaanssen, W. G. M., Menenti, M., Feddes, R. A., & Holtslag, A. A. M. (1998a). A remote sensing surface energy balance algorithm for land (SEBAL): 1. Formulation. *Journal of Hydrology*, *212–213*, 198–212.

Bastiaanssen, W. G. M., Molden, D. J., & Makin, I. W. (2000). Remote sensing for irrigated agriculture: Examples from research and possible applications. *Agricultural Water Management*, *46*, 137–155.

Bastiaanssen, W. G. M., Pelgrum, H., Wang, J., Ma, Y., Moreno, J. F., Roerink, G. J., et al. (1998b). A remote sensing surface energy balance algorithm for land (SEBAL): Part 2. Validation. *Journal of Hydrology*, *212–213*, 213–229.

Cellier, P., & Olioso, A. (1993). A simple system for automated long-term Bowen ratio measurement. *Agricultural and Forest Meteorology*, *66*, 81–92.

Choudhury, B. J., Idso, S. B., & Reginato, R. J. (1987). Analysis of an empirical model for soil heat flux under a growing wheat crop for estimating evaporation by an infrared-temperature based energy balance equation. *Agricultural and Forest Meteorology*, *39*, 283–297.

Coll, C., Caselles, V., Rubio, E., Valor, E., Sospedra, F., Baret, F., et al. (2002). Temperature and emissivity extracted from airborne multi-channel data in the ReSeDA experiment. *Agronomie*, *22*, 567–573.

Courault, D., Seguin, B., & Olioso, A. (2005). Review about estimation of evapotranspiration from remote sensing data: From empirical to numerical modeling approach. *Irrigation and Drainage Systems*, *19*.

François, C., Ottlé, C., & Prevot, L. (1997). Analytical parametrization of canopy directional emissivity and directional radiance in the thermal infrared. Application on the retrieval of soil and foliage temperatures using two directional measurements. *International Journal of Remote Sensing*, *18*(12), 2587–2621.

French, A., Schmugge, T. J., Kustas, W. P., Brubaker, K. L., & Prueger, J. (2003). Surface energy fluxes over El Reno, Oklahoma using high resolution remotely sensed data. *Water Resources Research*, *39*, 1164.

Gu, X. -F., Jacob, F., Hanocq, J. -F., & Tallet, N. (2000). Acquisition and processing of airborne thermal infrared data during the ReSeDA experiment. *Proceedings of the EGS2000 ReSeDA special session*. http://www.avignon.inra.fr/reseda/base/documents/reseda-report/RES-121.pdf

Hurtado, E., & Sobrino, J. A. (2001). Daily net radiation estimated from air temperature and NOAA-AVHRR data: A case study for the Iberian Peninsula. *International Journal of Remote Sensing*, *22*(8), 1521–1533.

Ines, A. V. M., Das Gupta, A. D., & Loof, R. (2002). Application of GIS and crop growth models in estimating water productivity. *Agricultural and Water Management*, *54*, 205–225.

Jacob, F., Gu, X. -F., Hanocq, J. -F., Tallet, N., & Baret, F. (2003). Atmospheric corrections of single channel and multidirectional airborne thermal infrared data: Application to the ReSeDA experiment. *International Journal of Remote Sensing*, *24*, 3269–3290.

Jacob, F., Olioso, A., Gu, X. F., Su, Z., & Seguin, B. (2002a). Mapping surface fluxes using airborne visible, near infrared, thermal infrared remote sensing data and a spatialized surface energy balance model. *Agronomie*, *22*, 669–680.

Jacob, F., Olioso, A., Weiss, M., Baret, F., & Hautecoeur, O. (2002b). Mapping short-wave albedo of agricultural surfaces using airborne PolDER data. *Remote Sensing of Environment*, *80*, 36–46.

Jacob, F., Weiss, M., Olioso, A., & French, A. N. (2002c). Assessing the narow-band to broad-band conversion to estimate visible, near infrared and shortwave apparent albedo from airborne PolDER data. *Agronomie*, *22*, 537–546.

Jia, L., Su, Z., Van der Hurk, B., Menenti, M., Moene, A., & De Bruin, H. A. R., et al. (2003). Estimation of sensible heat flux using the Surface Energy Balance System (SEBS) and ATSR measurements. *Physics and Chemistry of the Earth*, *28*(1–3), 75–88.

Kustas, W. P., & Norman, J. M. (1999). Evaluation of soil and vegetation heat flux predictions using a simple two-source model with radiometric temperatures for partial canopy cover. *Agricultural and Forest Meteorology*, *94*, 13–29.

Leroy, M., Hautecoeur, O., Berthelot, B., & Gu, X. -F. (2000). The airborne PolDER data during the ReSeDA experiment. *Proceedings of the EGS2000 ReSeDA special session*. http://www.avignon.inra.fr/reseda/base/documents/reseda-report/RES-111.pdf

Norman, J. M., Kustas, W. P., & Humes, K. S. (1995). Two source approach for estimating soil and vegetation energy fluxes in observations of directional radiometric surface temperature. *Agricultural and Forest Meteorology*, *77*, 263–293.

Olioso, A. (1995). Estimating the difference between brightness and surface temperatures for a vegetal canopy. *Agricultural and Forest Meteorology*, *72*, 237–242.

Olioso, A., Braud, I., Chanzy, A., Demarty, J., Ducros, Y., Gaudu, J. C., et al. (2002a). Monitoring energy and mass transfers during the Alpilles-ReSeDA experiment. *Agronomie*, *22*, 597–610.

Olioso, A., Hasager, C., Jacob, F., Wassenaar, T., Chehbouni, A., & Marloie, O., et al. (2002b). Mapping surface sensible heat flux from thermal infrared and reflectances data using various models over the Alpilles test site. In J. A. Sobrino (Eds.), *First international symposium on recent advances in quantitative remote sensing, 16–20 September 2002, Valencia, Spain* (pp. 450–457). España: Publicacions de la Universitat de València.

Olioso, A., Prevot, L., Baret, F., Chanzy, A., Braud, I., & Autret, H., et al. (1998). Spatial aspects in the Alpilles-ReSeDA project. In A. Marceau (Eds.), *Scaling and modeling in forestry: Application in remote sensing and GIS* (pp. 92–102). Québec: Université de Montréal.

Ortega-Farias, S., Olioso, A., Antonioletti, R., & Brisson, N. (2004). Evaluation of the Penman–Monteith model for estimating soybean evapotranspiration. *Irrigation Science*, *23*, 1–9.

Panda, R. K., Behera, S. K., & Kashyap, P. S. (2003). Effective management of irrigation water for wheat under stress conditions. *Agricultural Water Management*, *63*, 37–56.

Prévot, L., Baret, F., Chanzy, A., Olioso, A., et al. (1998). Assimilation of multisensor and multi-temporal remote sensing data to monitor vegetation and soil: The Alpilles-ReSeDA project. *IGARSS'98* (Seattle, WA, USA), IEEE, Ed., vol. CDRom, IEEE, IEEE (pp. E04-03).

Roerink, G. J., Su, Z., & Menenti, M. (2000). S-SEBI: A simple remote sensing algorithm to estimate the surface energy balance. *Physics and Chemistry of the Earth. Part B: Hydrology, Oceans and Atmosphere*, *25*(2), 147–157.

Seguin, B., & Itier, B. (1983). Using midday surface temperature to estimate daily evaporation from satellite thermal IR data. *International Journal of Remote Sensing*, *4*(2), 371–383.

Su, Z. (2002). The surface energy balance system (SEBS) for estimation of turbulent heat fluxes. *Hydrology and Earth System Sciences*, *6*(1), 85–99.

Van der Hurk, B. J. J. M., Bastiaanssen, W. G. M., Pelgrum, H., & Van Meijgaard, E. (1997). A new methodology for assimilation of initial soil moisture fields in weather prediction models using METEOSAT and NOAA data. *Journal of Applied Meteorology*, *36*, 1271–1283.

Wassenaar, T., Olioso, A., Hasager, C., Jacob, F., & Chehbouni, A. (2002). Estimation of evapotranspiration on heterogeneous pixels. In J. A. Sobrino (Ed.), *First international symposium on recent advances in quantitative remote sensing, 16–20 September 2002, Valencia, Spain* (pp. 458–465). España: Publications de la Universitat de València.

Weiss, M., Baret, F., Leroy, M., Hautecoeur, O., Bacour, C., Prévot, L., & Bruguier, N. (2002). Validation of neural net techniques to estimate canopy biophysical variables from remote sensing data. *Agronomie*, *22*, 547–553.